

Proposal and Evaluation of Attractor Perturbation-Based Rate Control for Stable End-to-End Delay

Midori Waki^(✉), Naoki Wakamiya, and Masayuki Murata

Graduate School of Information Science and Technology,
Osaka University, 1-5 Yamadaoka, Suita 565-0871, Japan
{m-waki,wakamiya,murata}@ist.osaka-u.ac.jp

Abstract. Due to the best-effort nature of the Internet, delay and delay jitter observed by a session always fluctuate, even if it generates CBR (Constant Bit Rate) traffic. Buffering at a host and packet scheduling at routers would solve the problem to some extent, but they require prior knowledge of delay variation and traffic characteristics. In this paper, we propose a novel rate control mechanism to achieve and maintain the target delay in the dynamically changing environment. Our proposal does not filter or conceal fluctuation, but it exploits fluctuation to accomplish the goal by using the attractor perturbation model derived from biological behavior. Through simulation experiments, we confirmed that our proposal could achieve and maintain the target delay when background traffic changed.

Keywords: Attractor perturbation · Rate control · End-to-end delay

1 Introduction

When there are multiple sessions sharing the same physical network resources, delay, delay jitter, and packet loss observed by a session always fluctuate, regardless of adopted protocol or characteristics of generated traffic. Since the origin of fluctuation includes changes in the number of sessions and the amount of traffic, the shadowing and fading of a wireless channel, rerouting of paths and others, that cannot be predicted or controlled by an individual session, researchers had made an effort to suppress fluctuations especially for delay-sensitive applications such as IPTV (Internet Protocol TeleVision) and video streaming.

Delay fluctuation is generally managed by a playout buffer at a receiver [1, 2]. A playout buffer defers video playout so that it can deposit the sufficient number of packets at the beginning and then provides a video player with buffered packets. As such, as far as packets arrive at a receiver before a buffer becomes empty, a video can be presented to a user without interruptions. However, delay and delay jitter are not predictable. Therefore, it is very likely that a buffer runs out of packets and a user experiences freezes. Increasing the number of packets

to buffer merely degrades the interactivity and timeliness of an application. For delay-sensitive applications, researchers proposed methods to control and reduce delay jitter by developing an intelligent packet scheduling algorithm at routers [3–7] and by multipath routing [8]. In [3], comparative analysis shows that packet scheduling at routers can reduce delay jitter even when buffering at a receiver cannot prevent freezes. However, it requires all intermediate routers from a server to a receiver to be equipped with the algorithm. On the contrary, a multipath routing method still relies on prior knowledge of delay variation, which is unpredictable in general. As a mechanism adopted at end systems, many rate control algorithms have been studied [9, 10]. They infer the network state by observing, for example, delay, delay jitter, and packet loss and regulate the sending rate to avoid network congestion. Although they can reduce the packet loss probability, they do not take into account the delay sensitivity of interactive applications.

As long as the network condition, such as the degree of congestion, can easily be predicted or estimated, it is trivial to control delay, delay jitter, and packet loss. However, the ever-increasing size, complexity, and dynamics of an information network prevent a control mechanism revealing the network condition even with active and aggressive probing. Going back to the simplest paradigm, given a complex system, what an end system can do is to apply a force and see how it reacts. Only if there exists the clear relationship between them, one can obtain the desired result by putting the appropriate force to a system. An answer can be found in biology, which has the long history of investigating and understanding complex systems, i.e. living organisms. The relationship is modeled by a mathematical expression, called an attractor perturbation model [11, 12]. It is derived from the relationship between fluctuations inherent in a biological system and its response against an external force. Biological systems are always exposed to internal and external fluctuation or noise caused by, for example, thermal fluctuation and phenotypic fluctuation. As a result, size, metabolic concentrations, and gene expression differ among cells cultured in the same medium and individuals are all different. Furthermore, gene expression of a cell dynamically changes to adapt to the surrounding conditions such as temperature, pH, and concentrations of chemical substances. Therefore, a cell is not always the same. It is considered that such fluctuation or diversity is a source of flexibility and adaptability of biological systems to environmental changes.

The attractor perturbation model explains how biological systems respond to environmental changes, which act as a force to trigger biological responses. Based on the model, given a change in the external force, the average of a measurable variable, such as the concentration of metabolic substances and the number of cells, shifts by the amount in proportional to the degree that a biological system fluctuates, i.e. the variance of the measurable variable. That is, more a biological system fluctuates, more it responds to the environmental change and alters its behavior.

Fluctuation is intrinsic to an information network as well. Then, the attractor perturbation model may hold in an information network and we can develop a control mechanism based on the model. When we regard a network as a

biological system and injected traffic as an external force imposed on a system, we can estimate how a network responds to a change in the injected traffic. More specifically, by adopting the end-to-end delay as a measurable variable of the attractor perturbation model, we can derive the appropriate amount of increase or decrease of the sending rate to achieve the desired end-to-end delay from the observed variance of delay. For example, assume that the measured end-to-end delay is larger than the desired delay. When the variance is large, it is enough to slightly decrease the sending rate to push down the delay to the desired level. On the contrary, aggressive rate control is required in a network with small fluctuation, which implies that a network is stable. With such a control mechanism based on the attractor perturbation model, efficient and effective rate adaptation can be accomplished without detailed information about a network system or tailored facilities.

The remainder of this paper is organized as follows. In Sect. 2, we briefly introduce the attractor perturbation model. In Sect. 3, we verify the attractor perturbation principle in an information network. In Sect. 4, we propose a novel rate control mechanism to achieve the stable end-to-end delay based on the attractor perturbation model. Then we conduct simulation experiments and evaluate the proposal in Sect. 5. Finally, Sect. 6 concludes the paper.

2 Attractor Perturbation Model

The attractor perturbation model represents the general relationship between inherent fluctuation and response in biological systems [11]. The following is a mathematical expression of the attractor perturbation model.

$$\langle w \rangle_{a+\Delta a} - \langle w \rangle_a = b\Delta a\sigma_a^2 \quad (1)$$

where $\langle w \rangle_a$ and σ_a^2 are the average and variance of measurable quantity w , e.g. protein concentration, under the force a , e.g. genetic mutation, respectively. Δa is a small change in the force and b is a constant coefficient. The equation indicates that a shift in the average of a measurable variable against a change in the force is proportional to the variance of the measurable variable. From Eq. (1), one can derive the following equation.

$$\langle w \rangle_{a+\Delta a} = \langle w \rangle_a + b\Delta a\sigma_a^2 \quad (2)$$

Equation (2) gives an estimate of an effect of increasing the force a to $a + \Delta a$ when the current average is $\langle w \rangle_a$ and the variance is σ_a^2 . From a viewpoint of control of the force, we can consider the following equation.

$$\Delta a = \frac{\langle w \rangle_{a+\Delta a} - \langle w \rangle_a}{b\sigma_a^2} \quad (3)$$

The equation gives the amount of change in the force, i.e. Δa , or the amount of force, i.e. $a + \Delta a$, to obtain the shifted average $\langle w \rangle_{a+\Delta a}$ from the current conditions $\langle w \rangle_a$, a , and σ_a^2 . This brings a basic idea of our proposal.

3 Attractor Perturbation Concept in Network

In this section, we verify that the attractor perturbation principle holds for a network system. We regard the end-to-end delay as the variable w and the rate of injected traffic as the external force a , and confirm the linear relationship between fluctuation and response, i.e. the variance of delay and the shift in the average delay.

3.1 Analytical Verification of Attractor Perturbation Concept in M/D/1 Model

First in this section, we prove the attractor perturbation principle in an M/D/1 queuing system assuming Poisson arrival of fixed-length packets. In the following, λ is the arrival rate, μ is the service rate, and $\rho = \lambda/\mu < 1$ is the traffic intensity or the load.

In [13], the author analyzes the mean time spent in an M/G/1 system, where the service time has a general distribution with mean $E(X)$. The first and second moment of time spent in an M/G/1 system are denoted by $E(T)$ and $E(T^2)$.

$$E(T) = \frac{\lambda}{2(1-\rho)}E(X^2) + E(X) \quad (4)$$

$$E(T^2) = \frac{\lambda}{3(1-\rho)} + \frac{\lambda^2}{2(1-\rho)^2}\{E(X^2)\}^2 + \frac{E(X^2)}{1-\rho} \quad (5)$$

Since the service time in an M/D/1 is constant, by substituting $E(X) = 1/\mu$ and $E(X^2) = 1/\mu^2$ into the above equations, we can obtain the mean $d(\lambda)$ and variance $\sigma^2(\lambda)$ of time spent in an M/D/1 system as functions of the arrival rate λ .

$$d(\lambda) = \frac{2\mu - \lambda}{2\mu(\mu - \lambda)} \quad (6)$$

$$\begin{aligned} \sigma^2(\lambda) &= E(T^2) - \{E(T)\}^2 \\ &= \frac{\lambda(4\mu - \lambda)}{12\mu^2(\mu - \lambda)^2} \end{aligned} \quad (7)$$

By differentiating $d(\lambda)$ with respect to λ we obtain

$$d'(\lambda) = \frac{1}{2(\mu - \lambda)^2} \quad (8)$$

Assuming that $\Delta\lambda$ is small, we further obtain the following relationship.

$$\frac{d(\lambda + \Delta\lambda) - d(\lambda)}{\Delta\lambda} = d'(\lambda) \quad (9)$$

$$\begin{aligned}
d(\lambda + \Delta\lambda) - d(\lambda) &= d'(\lambda)\Delta\lambda \\
&= \frac{1}{2(\mu - \lambda)^2}\Delta\lambda \\
&= \frac{6}{\rho(4 - \rho)}\sigma^2(\lambda)\Delta\lambda \tag{10} \\
&= b(\rho)\sigma^2(\lambda)\Delta\lambda \tag{11}
\end{aligned}$$

Therefore, the shift in the mean time spent in an M/D/1 queueing system is given as a product of the variance $\sigma^2(\lambda)$, the change $\Delta\lambda$ of arrival rate, and the coefficient $b(\rho)$. The coefficient $b(\rho)$ is depicted in Fig. 1. Whereas $b(\rho)$ exponentially decreases in the region of $\rho < 0.5$, it can be represented by a constant in the region of $\rho \geq 0.5$. We consider that rate adaptation is necessary especially when a network is moderately or highly loaded. Therefore, we can conclude that the attractor perturbation model is applicable to rate control in a moderately congested network system. In the next section, we verify the attractor perturbation concept in a packet-based network by simulation experiments using ns-2 [14].

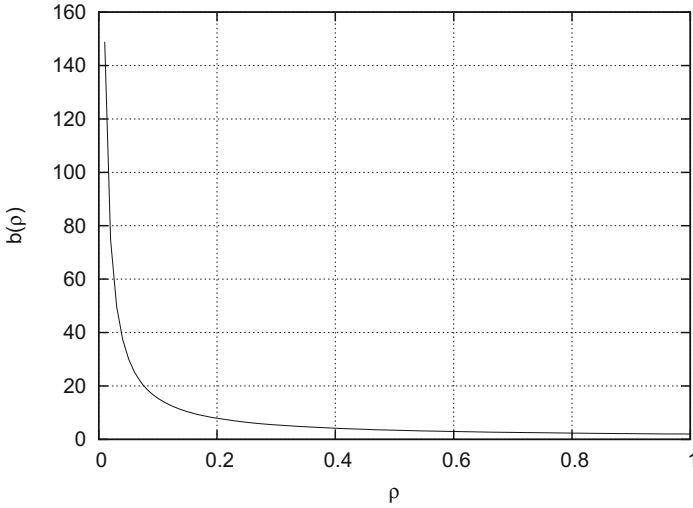


Fig. 1. variation of $b(\rho)$

3.2 Simulation-Based Verification of Linearity Between Fluctuation and Response

Figure 2 illustrates topology that we used for simulation. The dumbbell network models a bottleneck link of a network of arbitrary topology, which affects the end-to-end delay the most on a path. Two senders S_1 and S_2 are connected with

two receivers D_1 and D_2 , respectively, through routers E_0 and E_1 . All links are full-duplex. The bandwidth and the propagation delay of a link between routers E_0 and E_1 are 15 Mbps and 5 ms, respectively. Those of the other links are 1 Gbps and 1 ms.

A drop-tail FIFO buffer with the capacity of 1000 packets is deployed on each router. A CBR session called “session 1” is established between nodes S_1 and D_1 . We observe the one-way end-to-end delay on session 1 while changing the sending rate of UDP datagrams of a 1000-bytes payload. As background traffic, another UDP session, where the inter-arrival time of datagrams follows the exponential distribution and the payload size of a datagram is 1000 bytes, is set between nodes S_2 and D_2 . It is called “session 2”.

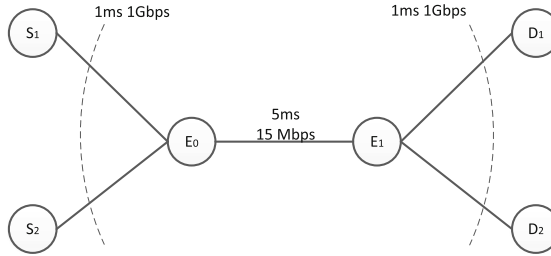


Fig. 2. Network topology used in simulation experiments

We observe the average $\langle w \rangle_a$ and variance σ_a^2 of one-way end-to-end delay of session 1 at the sending rate a Mbps. We prepared 10 traffic patterns of session 2 whose sending rate is 9 Mbps. For each of the pattern, we conducted 44 simulation experiments by increasing the sending rate a from 0.1 Mbps to 4.5 Mbps by 0.1 Mbps, i.e. $\Delta a = 0.1$. Then, from averages and variance obtained from 440 simulation experiments, we derive 430 pairs of σ_a^2 and $\langle w \rangle_{a+0.1} - \langle w \rangle_a$, i.e. $\sigma_{1.0}^2$ and $\langle w \rangle_{1.1} - \langle w \rangle_{1.0}$.

If the attractor perturbation principle holds, there exists the linear relationship between $\Delta a \cdot \sigma_a^2$ and $\langle w \rangle_{a+\Delta a} - \langle w \rangle_a$ as Eq. (1) indicates. 430 pairs of $0.1\sigma_a^2$ and $\langle w \rangle_{a+0.1} - \langle w \rangle_a$ are plotted on Fig. 3 as crosses. The figure shows the positive correlation between $0.1\sigma_a^2$ and $\langle w \rangle_{a+0.1} - \langle w \rangle_a$ and we can confirm the attractor perturbation principle in a packet-based network. When the sending rate of CBR session is low, there is little chance for packets to experience buffering at routers. As a result, the variance becomes small and the small increase of sending rate does not affect the delay much. Therefore, when the variance is small, the shift in the average delay becomes small as well. On the contrary, as the sending rate increases, the number of packets buffered at routers begins to fluctuate. It leads to both of the larger delay and the variance. Consequently, we observe the linear relationship between the variance and the shift in delay.

The proportional constant of the relationship between $0.1\sigma_a^2$ and $\langle w \rangle_{a+0.1} - \langle w \rangle_a$ corresponds to the coefficient b of Eq. (1). In Fig. 3, we show an approximate

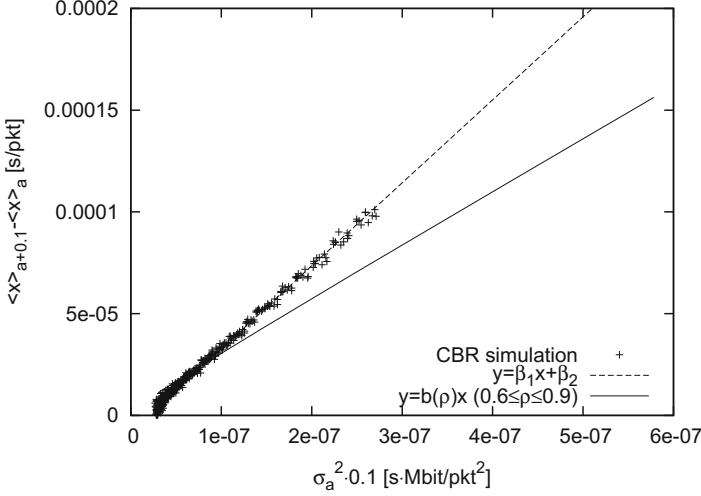


Fig. 3. Attractor perturbation relationship of CBR traffic

line $y = \beta_1 x + \beta_2$ obtained by the least squares approximation where x is $0.1\sigma_a^2$ and y is $\langle w \rangle_{a+0.1} - \langle w \rangle_a$. The slope, i.e. β_1 , of the line can be regarded as the coefficient b , and its value is 407.63. The load ρ at the variance σ_a^2 is calculated by λ/μ , where μ is the service rate of the bottleneck link and λ is the arrival rate when the variance is σ_a^2 . Therefore, ρ depends on σ_a^2 and the x-axis can be mapped to ρ . In Fig. 3, $y = b(\rho)x$ in the range of $0.6 < \rho < 0.9$ is depicted. To compare the analytical result of an M/D/1 system discussed in the previous section, we convert $b(\rho)$ to $\frac{750}{\rho(4-\rho)}$ by $\Delta\lambda = \frac{\Delta a \times 10^6}{8000}$ in Eq. (10). Although it is not a linear function due to the variation of ρ , the slope $b(\rho)$ is about 300 on average in the range of $0.6 < \rho < 0.9$. As shown in Fig. 3, there is a difference in slope between the analytical result and the simulation result. For the same variance, the shift $\langle w \rangle_{a+0.1} - \langle w \rangle_a$ is larger in the simulation than in the analysis. Given the variance σ_a^2 , the load on a network in the case of the analysis, which can be derived from Eq. (7), is smaller than that of the simulation, which can be derived as $(a+9)/15$ considering that the amount of background traffic is 9 Mbps and the capacity of the bottleneck link is 15 Mbps. In general, when the sending rate increases, the end-to-end delay becomes larger in a congested network than in an unloaded network. Consequently, the growth rate or the slope is larger in the simulation than in the analysis. In Sect. 5, we used three alternatives of coefficient b , that is, 407.63, 300, and $b(\rho)$, to evaluate its influence.

4 Attractor Perturbation-Based Rate Control Mechanism

In this section, we propose a novel rate control mechanism based on the attractor perturbation model. We regard the delay as the measurable variable x and the

sending rate as the force a and derive the appropriate sending rate to accomplish the target delay under the fluctuating environment.

We consider an application which communicates at least for several minutes. An application specifies the target one-way delay T s, the maximum sending rate a_{max} Mbps, and the minimum sending rate a_{min} Mbps. RTP/UDP and RTCP/UDP are employed and the sending rate is adjusted by adapting a transmission interval of RTP packets. Figure 4 illustrates how packets are exchanged and the sending rate is adjusted.

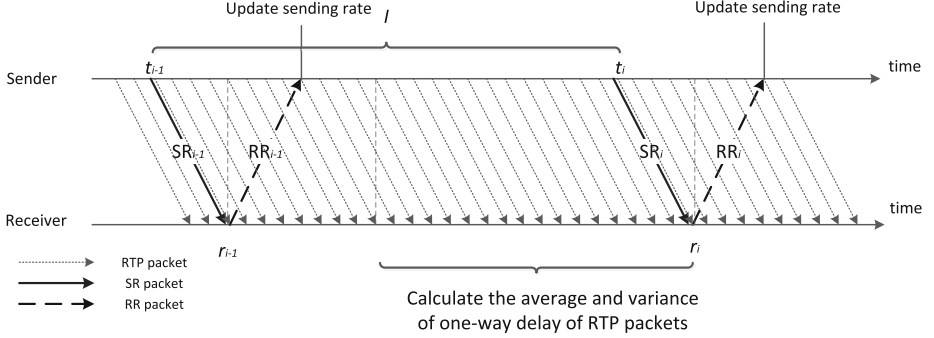


Fig. 4. Outline of proposal

At the beginning of a session, a sender sends RTP packets at the minimum rate a_{min} Mbps. Besides this, to obtain average delay d_i and variance v_i^2 a sender sends Sender Report (SR) packets at regular intervals of I s. The i -th SR packet emitted at time t_i s carries the information t_{i-1} , i.e. the instance when the $(i-1)$ -th SR packet was sent, in its header. A receiver sends back a Receiver Report (RR) packet in response to a SR packet.

Now consider that a receiver receives the i -th SR packet at r_i s. It calculates the average d_{i-1} and variance v_{i-1}^2 of one-way delay of RTP packets received from $t_{i-1} + 2(r_i - t_i)$ s to r_i s (see Fig. 4). Since packets received from r_{i-1} s to $t_{i-1} + 2(r_i - t_i)$ s are sent before the rate adaptation initiated by reception of the $(i-1)$ -th RR packet by a sender, they are excluded from the calculation. Then, the receiver sends a RR packet carrying the derived average and variance in an extended header.

On receiving the RR packet, the sender first calculates the amount Δa Mbps of rate change by substituting the received values, the target delay T , and the coefficient b to the following equation.

$$\Delta a = \frac{T - d_{i-1}}{bv_{i-1}^2} \quad (12)$$

Next, the sender updates the sending rate to a_{new} Mbps, which is derived from the following equation.

$$a_{new} = \min\{a_{max}, \max(a_{min}, a + \Delta a)\} \quad (13)$$

If a sender does not receive any of the $(i - n)$ -th RR packets ($n \in 1, 2, 3$) by $t_i + 1 + I$ s, i.e. an instance to send the i -th SR packet, it considers that a network is considerably congested. Then, the sender reduces the sending rate by half and quits sending the i -th SR packet at $t_i + 1 + I$ s. After additional I s, if the sender receives any RR packets until then, it sends the i -th SR packet carrying $t_i - 1 + I$ s in an extended header to a receiver. On receiving the SR packet, the receiver calculates the average and variance of delay of RTP packets received from $t_{i-1} + I + 2(r_i - t_i)$ s to r_i s and sends a RR packet to the sender.

5 Evaluation

In this section, we evaluate our proposal through simulation experiments. We first describe a simulation model and measures. Then, we verify that our proposal can achieve and maintain the target delay even when background traffic changes.

5.1 Simulation Setting

We used the dumbbell topology depicted in Fig. 2 and set a UDP session same as Sect. 3.2. The amount of background traffic on session 2 is increased from 9 Mbps to 10.5 Mbps, in terms of load, from 0.6 to 0.7, at 200 s in a simulation run of 400 s. We employ our proposal on session 1 established between nodes S_1 and D_1 . The size of a RTP packet including RTP, UDP, and IP headers is set at 1000 bytes. The sizes of a SR packet and a RR packet including an IP header are 64 and 72 bytes, respectively. The maximum sending rate a_{max} and the minimum sending rate a_{min} of our proposal are 15.0 Mbps and 0.1 Mbps, respectively. The interval I of SR packets is 10 s. The target delay is set at 8.2 ms, which is the one-way delay observed in the simulation experiments of the case of $\rho = 0.8$ in Sect. 3.2. Parameters used in evaluations are summarized in Table 1.

In order to evaluate the influence of the coefficient b , we conduct simulation experiments with $b = 300, 407.63$, and function $b(\rho)$. $b(\rho)$ enables dynamic adaptation of b with respect to the load condition. In the case of $b(\rho)$, we assume that a sender node can know the current load ρ of a network to derive the appropriate rate change Δa , whereas it is not possible to have the accurate and up-to-date information about the load condition of a network in an actual situation. More specifically, at t_i s, when a sender sends the i -th SR packet, the average load ρ_i on the bottleneck link between t_{i-1} s and t_i s is given and substituted into $b(\rho_i)$.

For comparison purposes, we additionally conduct simulation experiments for the cases of CBR traffic. In those cases, session 1 generates CBR traffic of 3 Mbps or 0.8 Mbps using RTP and RTCP. Note that a pair of SR and RR packets is sent every 10 s, but it is not used for rate control. We denote a case of CBR traffic with sending rate of 3 Mbps as CBR 3 Mbps and that of 0.8 Mbps as CBR 0.8 Mbps.

Table 1. Parameter setting

Parameter	Value
a_{min}	0.1 [Mbps]
a_{max}	15 [Mbps]
Interval I of SR packets	10 [s]
T	8.2 [ms]
b	300, 407.63

5.2 Evaluation Measures

To evaluate how our proposal achieves and maintains the target delay, we introduce the mean square error, the coefficient of variation, and the delay jitter defined in the following. We consider the first control interval after the initial transient state as the 0-th interval.

Mean Square Error. We evaluate the closeness to the target delay by the mean square error. First, we calculate the average delay T_i of successfully received RTP packets that are sent in the i -th control interval from t_i s to t_{i+1} s. Note that T_i is not equal to d_i , which is the average delay defined in Sect. 4. Then, we obtain the mean square error M as follows.

$$M = \frac{1}{n+1} \sum_{i=0}^n (T_i - T)^2 \quad (14)$$

Here T is the target delay, n is the number of SR packets sent in the whole simulation time. Therefore, T_n is the average delay of RTP packets that are sent from t_n s to the end of the simulation. A small M means that the average delay is close to the target delay in most of cases.

Coefficient of Variation. We evaluate the stability of the average delay by the coefficient of variation. We calculate the mean \bar{T} and the standard deviation σ^2 of the average delay in the simulation as below.

$$\bar{T} = \frac{1}{j+1} \sum_{i=0}^n T_i \quad (15)$$

$$\sigma^2 = \sqrt{\frac{1}{n+1} \sum_{i=0}^n (T_i - \bar{T})^2} \quad (16)$$

Then we obtain the coefficient C of variation as follows.

$$C = \frac{\sigma^2}{\bar{T}} \quad (17)$$

A small C means that the average delay is kept constant and stable.

Delay Jitter. We define the delay jitter J as follows.

$$J = \max_{0 \leq i \leq n} \{|T_i - T|\} \quad (18)$$

The delay jitter is the maximum difference between the target delay T and the average delay T_i .

5.3 Evaluation Results

First we show an example of temporal variations in Figs. 5 and 6. In Fig. 5, variations of average delay T_i against the simulation time are depicted. In Fig. 6, variations of averaged sending rate per control interval are depicted. All results in the figures are obtained from simulation experiments with the identical background traffic pattern.

As shown in Fig. 5, CBR 3.0 Mbps results in the average delay close to the target delay at the beginning, but the delay becomes larger after the increase of background traffic. On the contrary, the average delay of CBR 0.8 Mbps is as low as the target delay from 200 s, whereas it is smaller than the target delay in the first half on the simulation run. Regarding our proposal, independently of the setting of coefficient b , the average end-to-end delay stays close to the target delay except for the period right after the sudden load increase. In the case of $b = 300$ for example, a sender node tries to decrease the sending rate on reception of a RR packet from a receiver node at 201 s. However, the decrease is only 0.33 Mbps at that time as shown in Fig. 6. It is because the delay and variance informed by the RR packet are derived from RTP packets sent before the load increase. At the next timing of rate control at 211 s, delay and variance have grown much

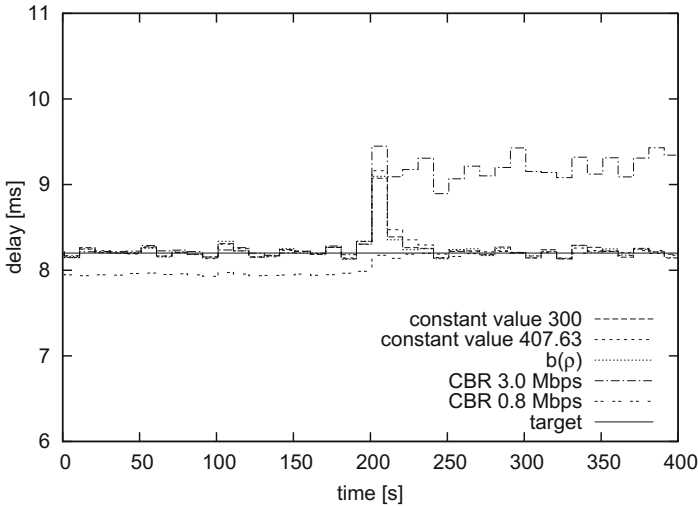


Fig. 5. Comparison of average delay

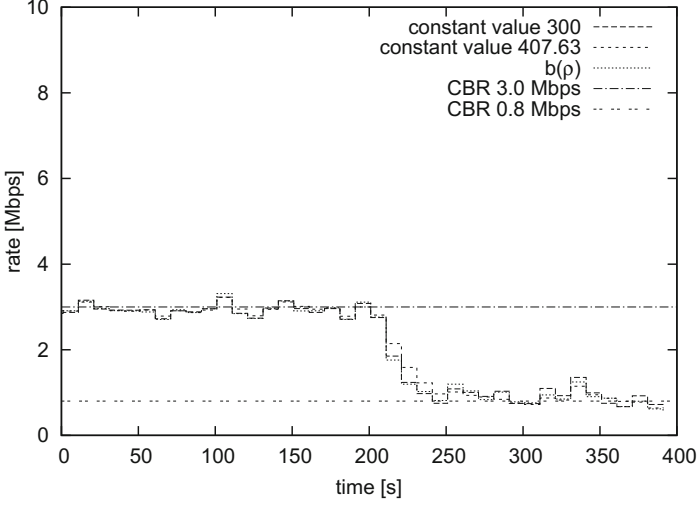
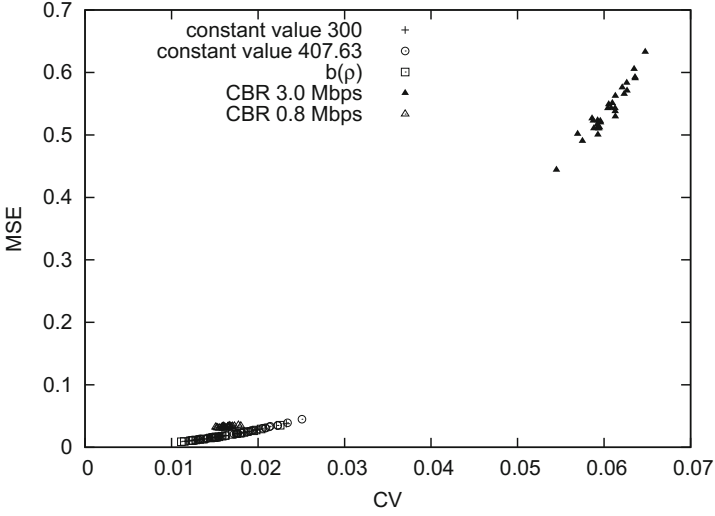


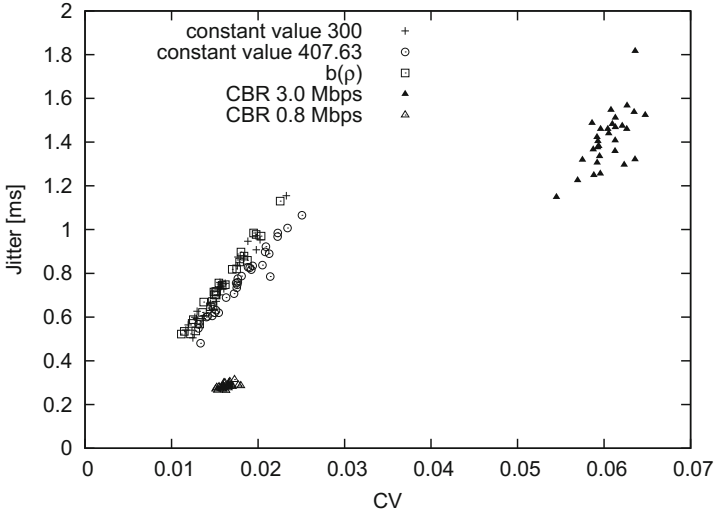
Fig. 6. Comparison of sending rate

to 9.07 ms and 3.23 ms² respectively. Then, the amount of decrease derived at the sender node becomes 0.90 Mbps. As a result of drastic rate reduction, the obtained end-to-end delay approaches the target delay again. The instantaneous increase of delay is basically unavoidable, but the duration can be shortened by a shorter control interval, that is, frequent rate control. However, too short control interval decreases the accuracy of variance derivation as a statistic and a sender node cannot precisely capture the fluctuation of a network. We should emphasize here that setting of constant value b does not affect the performance of our proposal very much. It suggests that the prior knowledge or parameter tuning, such that we did in Sect. 3.2, is not necessary.

Figure 7 summarizes results of all simulation experiments conducted 30 times for each settings. Figure 7(a,b) show the relationship between the coefficient of variation and the mean square error, and that between the coefficient of variation and the delay jitter, respectively. In both figures, the closer the point is to the origin, the more stable the end-to-end delay is around the target delay. Figure 7 shows that points of our proposal overlap with each other independently setting of the coefficient b and they are in the lower left region. MSE of our proposal is smaller than that of CBR 0.8 Mbps and much smaller than that of CBR 3.0 Mbps. On the other hand, our proposal results in larger coefficient of variation in some cases and larger delay jitter in all cases than CBR 0.8 Mbps. A reason is that the average delay does not change much before and after the load increase due to the low sending rate with CBR 0.8 Mbps. In contrast, our proposal suffers from the instantaneous increase of delay after the load increase. It makes the delay jitter larger than that of CBR 0.8 Mbps and affects the coefficient of variation as well. From a practical view point, the delay jitter of as much as 1.2 ms on a session of the propagation delay of 15 ms is small enough.



(a) Coefficient of variation and mean square error



(b) Coefficient of variation and delay jitter

Fig. 7. Performance comparisons

In summary, we can conclude that our proposal can accomplish the stable end-to-end delay facing to the sudden load increase except for the instantaneous growth of delay right after the increase. We further showed that the setting of coefficient b did not influence rate control very much, which supports our motivation not to rely on the prior or detailed knowledge about characteristics

of a network. That is, our proposal is insensitive to parameter setting as can be seen in the flexibility and robustness of biological systems.

6 Conclusion and Future Work

In this paper, as an example of application of the attractor perturbation model, we propose a novel rate control mechanism to achieve and maintain the target delay in the dynamically changing environment. We first proved that the attractor perturbation principle held in a packet-based network as well as a general M/D/1 queuing system. Next through simulation experiments, we confirmed that our proposal could achieve the goal and more interestingly the setting of coefficient b did not influence the performance of proposal very much.

As future work, we are going to conduct further evaluation to verify the insensitivity of our proposal to characteristics of a network including the size, topology, and competing sessions and their protocols. Furthermore, we plan the comparison with other non-bio-inspired mechanisms for delay jitter suppression. Some mechanisms such as a playout buffer can be incorporated with our proposal. From a view point of the attractor perturbation principle, the behavior of other incorporated mechanism is another origin of fluctuation of a network system. As such, it only changes the variance of end-to-end delay observed by our rate control mechanism. Then, we can expect that our proposal can work well without any tuning, modification, or extension.

Acknowledgement. This research was supported in part by Grand-in-Aid for Scientific Research (B) 22300023 of the Ministry of Education, Culture, Sports, Science and Technology, Japan.

References

1. Atzori, L., Lobina, M.: Playout buffering in IP telephony: a survey discussing problems and approaches. *IEEE Commun. Surv. Tutor.* **8**, 36–46 (2006)
2. Fujimoto, K., Ata, S., Murata, M.: Adaptive playout buffer algorithm for enhancing perceived quality of streaming applications. *Telecommun. Syst.* **25**, 259–271 (2004)
3. Kadur, S., Golshani, F., Millard, B.: Delay-jitter control in multimedia applications. *Multimedia Syst.* **4**, 30–39 (1996)
4. Verma, D., Zhang, H., Ferrari, D.: Delay jitter control for real-time communication in a packet switching network. In: *Proceedings of IEEE TRICOMM'91*, pp. 35–43, April 1991
5. Mansour, Y., Patt-Shamir, B.: Jitter control in QoS networks. *IEEE/ACM Trans. Network.* **9**, 492–502 (2001)
6. Pedrasa, J., Festin, C.: Value-based utility for jitter management. In: *Proceedings of IEEE Region 10 Conference*, pp. 1–5, November 2006
7. Hay, D., Scalosub, G.: Jitter regulation for multiple streams. *IEEE/ACM Trans. Algorithms* **6**, 1–19 (2009)
8. Okuyama, T., Yasukawa, K., Yamaoka, K.: Proposal of multipath routing method focusing on reducing delay jitter. In: *Proceedings of IEEE Pacific Rim Conference*, pp. 296–299, August 2005

9. Busse, I., Deffner, B., Schulzrinne, H.: Dynamic QoS control of multimedia applications based on RTP. *Comput. Commun.* **19**(1), 49–58 (1996)
10. Sun, Y., Tsou, F., Chen, M.: Predictive flow control for TCP-friendly end-to-end real-time video on the internet. *Comput. Commun.* **25**, 1230–1242 (2002)
11. Sato, K., Ito, Y., Yomo, T., Kaneko, K.: On the relation between fluctuation and response in biological systems. *Nat. Acad. Sci.* **100**, 14086–14090 (2003)
12. Leibnitz, K., Murata, M.: Attractor selection and perturbation for robust networks in fluctuating environments. *IEEE Netw.* **24**, 14–18 (2010)
13. Shanthikumar, J.: On reducing time spent in M/G/1 systems. *Eur. J. Oper. Res.* **9**, 286–294 (1982)
14. The network simulator ns-2. <http://www.isi.edu/nsnam/ns/>

Bio-Inspired Models of Network, Information, and
Computing Systems

7th International ICST Conference, BIONETICS 2012,
Lugano, Switzerland, December 10--11, 2012, Revised
Selected Papers

Di Caro, G.A.; Theraulaz, G. (Eds.)

2014, XI, 323 p. 125 illus., Softcover

ISBN: 978-3-319-06943-2